Tetrahedron Letters 52 (2011) 5315–5318

Contents lists available at SciVerse ScienceDirect

Tetrahedron Letters

journal homepage: www.elsevier.com/locate/tetlet

Highly-strained cyclophanes bearing both photo- and electro-active constituents

Andrew C. Benniston [a,*], Anthony Harriman [a], Songjie Yang [a], Ross W. Harrington [b]

[a] Molecular Photonics Laboratory, School of Chemistry, Newcastle University, Newcastle upon Tyne, NE1 7RU, UK
[b] Crystallography Centre, School of Chemistry, Newcastle University, Newcastle upon Tyne, NE1 7RU, UK

ARTICLE INFO

Article history:
Received 2 June 2011
Revised 26 July 2011
Accepted 2 August 2011
Available online 7 August 2011

Keywords:
4,4′-Bipyridinium
Azobenzene
Macrocycle
Redox center
X-ray structure
Isomerization

ABSTRACT

The synthesis of a highly-strained cyclophane comprising azobenzene and methyl viologen units was achieved by coupling 3,3′-dihydroxy-4,4′-bipyridine with azobenzoic acid in CH_2Cl_2. The molecular structure, determined by single-crystal X-ray crystallography, shows that the azobenzene N=N unit adopts the *trans* conformation and that the bipyridinium unit is twisted. The cyclic voltammogram recorded for the target compound displays an irreversible wave at −0.37 V vs Ag/AgCl, associated with the one-electron reduction of the bipyridinium subunit. A further wave is seen at $E_{1/2} = -1.52$ V versus Ag/AgCl and is assigned to one-electron reduction of the azobenzene group. Visible light illumination of the azobenzene chromophore in CH_3CN triggers *trans* to *cis* isomerization but the process is irreversible.

© 2011 Elsevier Ltd. All rights reserved.

Functionalized cyclophanes represent a class of cyclic structures[1] incorporating one or more units that are capable of activation by external stimulus (e.g., light,[2] protonation,[3] cation binding,[4] electrochemical oxidation[5]). In many cases, the cyclophane is a relatively small feature in a more elaborate structure, but its activation triggers a cascade of events that may, for example, alter the shape,[6] hydrophobicity,[7] colour,[8] and/or H-bond affinity[9] of the superstructure. Certainly the light-driven molecular shuttling observed in rotaxane systems is a prime example of directed large-scale structural alteration.[10] Identification of suitable molecular building blocks capable of selective activation is critical, with the azobenzene subunit[11] and viologen (4,4′-bipyridinium dication)[12] group representing two heavily used photo- and redox-active moieties, respectively. Selective light activation of azobenzene is known to facilitate N=N *trans* to *cis* isomerization, which is accompanied by slow (seconds to hours) thermal reversion to the *trans* form.[13] The large-scale structural change that takes place is put to good use in many molecular electronics applications.[14] Likewise, the two-electron reduction of methyl viologen (*N,N*′-dimethyl-4,4′-bipyridinium dication) is very well understood. In the ground state, the two pyridinium rings of the dication are twisted around the connecting C–C bond, but upon one-electron reduction they become planar.[15] Previously, we demonstrated that the reduction potentials for a series of constrained viologen derivatives were highly dependent on the length of the tether linking the two pyridinium rings.[16] The results, in fact, can be used to argue that switching of the dihedral angle subtended between the pyridinium rings by ca. 27° will alter the reduction potential by some 560 mV. Such a substantial difference in reduction potential may be put to good effect in a variable resistor construct,[17] where an alteration in dihedral angle would retard (act as a gate to) electron flow in one dimension (Fig. 1). To this end, linking together a viologen subunit and an azobenzene unit into a single cyclophane structure seems to meet the correct design principle for a light-activated variable resistor. If the spacer between the two units is sufficiently short, light-induced *trans* to *cis*

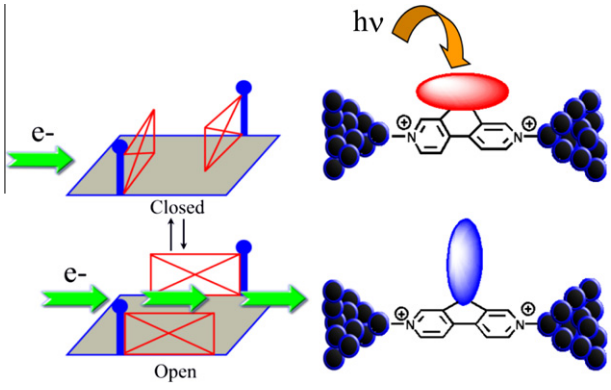

Figure 1. Pictorial representation of a light-activated variable resistor in a molecular construct where the open gate facilitates electron flow but no current passes when the gate is closed.

* Corresponding author.
E-mail address: a.c.benniston@ncl.ac.uk (A.C. Benniston).

0040-4039/$ - see front matter © 2011 Elsevier Ltd. All rights reserved.
doi:10.1016/j.tetlet.2011.08.013

isomerization should twist the bipyridinium group. The preparation and properties of the first prototype of this new class of molecule, **AZV**, is presented here.

Scheme 1 illustrates the methodology employed for preparation of **AZV** starting from the known 3,3′-dihydroxy-4,4′-bipyridine (**2**).[18] Cyclization of **2** with the dicarboxylic acid derivative **1**[19] in dry CH_2Cl_2, using DCC as the coupling agent, produced two main products after column chromatography (silica gel, CH_2Cl_2/acetone 4:1 then 2:1) purification. The ^1H NMR spectra recorded for these two compounds were markedly disparate, especially with respect to the most downfield resonances associated with the bipyridinium subunit. For one product, a broad singlet was observed at $\delta = 8.70$ and a doublet at $\delta = 8.55$ ($J = 3.5$ Hz). In the second case, a well resolved doublet ($\delta = 8.73$, $J = 4.8$ Hz) and a singlet ($\delta = 8.66$) were observed. The mass spectrum indicated that, in fact, the first fraction collected by column chromatography was the [1+1] adduct (**3**)[20] while the second fraction was the [2+2] product (**4**).[21]

The final step of a supposedly straightforward dialkylation of the 4,4′-bipyridine group proved to be frustratingly difficult. The tried and tested method is to alkylate with CH_3I followed by ion exchange to convert the water-soluble iodide salt to the organic-soluble hexafluorophosphate derivative. Under such conditions, the attempted conversion of **3** to **AZV** failed, and only the *N*-alkylated version of **2** was evident from the ^1H NMR spectrum. Eventually, the source of the problem was found to be water hydrolysis of the iodide salt of **AZV**, most likely enhanced by the close proximity of the positive charge to the ester as discussed by Engbersen et al.[22] To overcome this problem, the direct alkylation of **3** using methyl triflate in CH_3CN, followed by multiple recrystallization, afforded the desired compound as a red solid, which was soluble in CH_3CN and acetone.[23] The attempted alkylation of **4** unfortunately afforded a mixture of products presumably representing the mono- to tetra-cationic species. Multiple recrystallization failed to isolate only one compound, while column chromatographic separation was ruled out owing to the susceptibility of these compounds to hydrolysis.

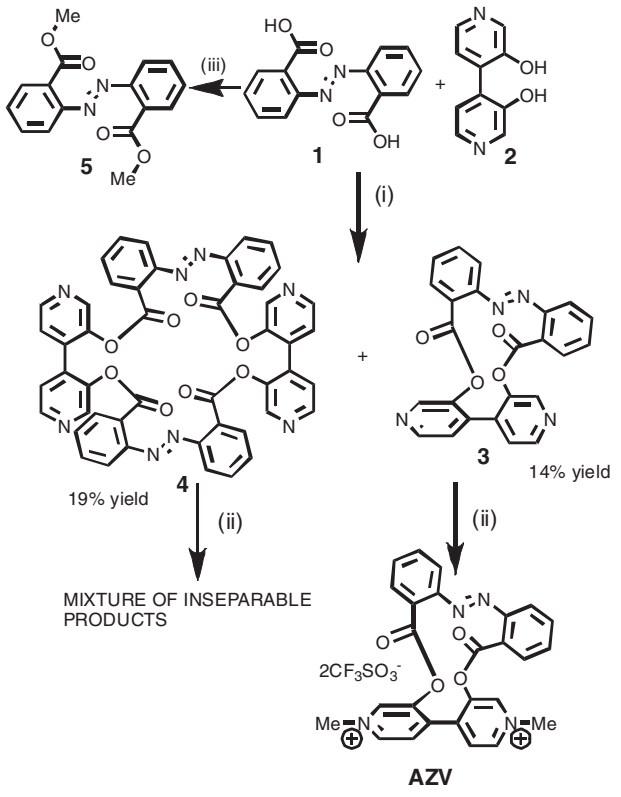

Scheme 1. Reagents and Conditions: (i) CH_2Cl_2, DCC, room temperature, (ii) $MeSO_3CF_3$, CH_3CN, room temperature, (iii) MeOH, H^+, reflux.

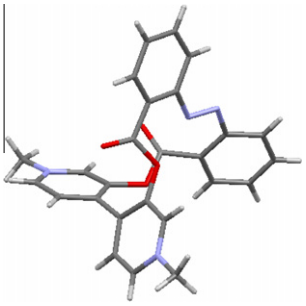

Figure 2. X-ray molecular structure determined for **AZV**. Triflate ions and a solvent molecule are omitted for clarity.

Single-crystals obtained by slow vapor diffusion of Et_2O into a solution of **AZV** in CH_3CN were suitable for X-ray diffraction analysis.[24] The molecular structure obtained is shown in Figure 2. The bipyridinium cation is highly twisted, the dihedral angle between the two planes created using each ring as a reference point is 67.6°. The azobenzene group is also distorted from planarity, the dihedral angle between the two planes of the two aromatic rings is 39.6°. The obvious steric strain inherent to this cyclophane can be exemplified by the close distance (3.2 Å) between the two oxygen atoms of the bipyridinium subunit. The energy-minimized geometry computed by DFT calculations for the isolated molecule differs markedly from the X-ray structure. The most notable difference relates to the reduced dihedral angle of 9.6° between the pyridinium cations. In this case, most of the strain is taken up by the diazobenzene unit, where the dihedral angle is 27°, with the oxygen atoms being forced into surprisingly close (4 Å) proximity. There is a similar trend in the computed geometry for the [2+2] cyclophane where the viologen unit tends toward planarity but the azobenzene residue is heavily distorted. This latter structure is interesting in as much as the four carbonyl oxygen atoms point into the interior of the cavity in the form of two pairs, with O–O distances of 2.4 and 4.0 Å.

The electrochemical behavior of **AZV** was explored using cyclic voltammetry in dry CH_3CN (0.2 M TBATFB as the background electrolyte) at a glassy carbon working electrode. A typical voltammogram, restricted to −1.70 V vs Ag/AgCl, is shown in Figure 3. The first point to note is the irreversible peak seen at −0.37 V (vs Ag/AgCl) on reductive scans which represents the one-electron reduction of the viologen unit. The position of this peak is as expected for a slightly strained viologen derivative. However, the re-oxidation wave is not observed even at faster scan rates ($\leqslant 2$ V s^{-1}) or when the reductive scan is switched at −0.7 V (vs Ag/AgCl), and this situation is most unusual for a viologen derivative. Moreover, the second reduction wave normally observed for viologen derivatives, which forms the neutral species and is expected at ca. −1 V (vs Ag/AgCl), is absent for **AZV**, at least over the anticipated potential range. It was noted for this first reduction that, as well as the normal increase in cathodic current, the peak potential undergoes a gradual shift to more negative potentials on raising the scan rate (see Supplementary data). Such behavior is consistent with a fast chemical reaction accompanying the addition of an electron (i.e., an ec mechanism). The irreversible electrochemistry is not caused by the 2,2′-substituents, since reversible reduction steps have been reported for a series of dialkoxy strapped viologens,[16] but appears to be unique to this compound. That the first reduction peak is associated with the viologen unit was confirmed by recording the cyclic voltammogram for **3** under identical conditions.

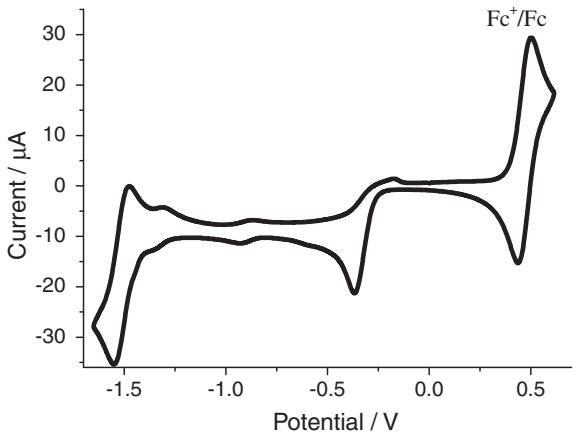

Figure 3. Cyclic voltammogram recorded for **AZV** in dry CH_3CN (0.2 M TBATFB) at a glassy carbon working electrode and versus an Ag/AgCl reference. Scan rate = 50 mV s^{-1}.

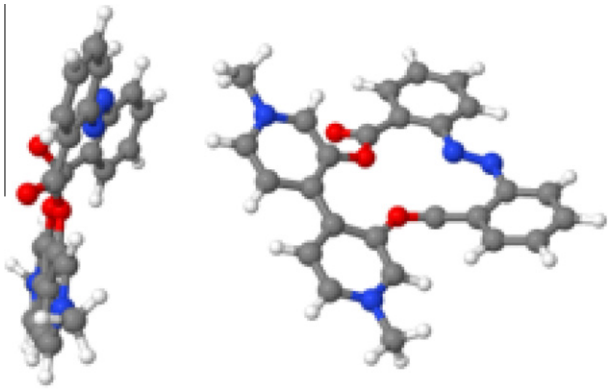

Figure 4. Computed structure for the monocation radical required to permit electron delocalization, and showing the severe distortion at the viologen units that leads to the banana-shaped geometry.

For **AZV**, a second wave is evident at $E_{1/2} = -1.52$ V ($\Delta E = 70$ mV) vs Ag/AgCl. The scan rate dependence for this latter wave (see Supplementary data) is consistent with that expected for a quasi-reversible step. In an attempt to assign the molecular group responsible for this latter wave, cyclic voltammograms were recorded for the methyl ester **5** under identical conditions (see Supplementary data). Here, the voltammogram is dominated by a quasi-reversible wave at $E_{1/2} = -1.05$ V ($\Delta E = 80$ mV) vs Ag/AgCl and an irreversible wave at $E_{red} = -1.41$ V vs Ag/AgCl. As noted for other azobenzene compounds, the reverse peak for this latter wave is located at −0.76 V vs Ag/AgCl, and becomes more pronounced at higher scan rates. On the basis of the combined electrochemistry results, it seems most likely that the second reductive wave seen for **AZV** corresponds to the reversible addition of one electron to the azobenzene group. Steric strain imposed by the cyclophane structure makes this step much more difficult than for the isolated subunit.

A DFT (B3LYP, 6-311G) calculation performed on the energy-minimized structure generated for **AZV** (see Supplementary data) is consistent with the LUMO lying on the viologen moiety, as deduced by cyclic voltammetry. Calculations further indicate that the neutral viologen can be formed, albeit with a distorted (i.e., banana-shaped) geometry that will certainly push the second reduction potential towards more negative values. As such, the absence of a re-oxidation peak for the monocation radical must arise because of the instability of this species. Because the potential is modest, full bond cleavage is most unlikely and instead we attribute the accompanying chemical reaction to radical attack at the azo centre of a second molecule. Indeed, azobenzene is known to be susceptible to addition reactions under electrochemical conditions. For **AZV**, we surmise that addition of the first electron generates the monocation radical whereby the radical center is not fully delocalized but, due to steric constraints, is localized on one pyridine ring (Fig. 4). This radical attacks an azobenzene group, although the cyclophane arms probably prevent intramolecular reaction.

The absorption spectrum recorded for the control compound **5** in CH_3CN shows a broad, Gaussian-shaped profile with a maximum at 442 nm (Full-Width at Half Maximum (FWHM) = 96 nm). This band is characterized by a relatively small molar absorption coefficient at the peak maximum and bears all the recognized hallmarks of an n–π* electronic transition associated with the azobenzene unit.[25] This band is extremely important in the context of molecular photonic devices since it is responsible for the *trans* to *cis* isomerization. There is also a more intense π,π* transition centered at about 330 nm. In contrast, the absorption spectrum recorded for **AZV** in CH_3CN is more complex and not so easily interpreted (Fig. 5). The low energy region comprises at least two overlapping bands (see Supplementary data) with maxima at 412 nm (FWHM = 51 nm) and 457 nm (FWHM = 65 nm). This latter band is assigned to the azobenzene-based n–π* electronic transition by reference to the cyclophane **3**. The broad band occurring at higher energy is attributed tentatively to a charge-transfer transition between the azobenzene and viologen subunits; this particular transition is absent in **3**. The relatively intense absorption transition identified for the azobenzene unit is also present for **AZV** but overlaps somewhat with corresponding π,π* transitions localized on the viologen unit and appearing at 283 nm. An important finding from these studies is that the n,π* transition for **AZV** occurs at low energy, although overlapping with one or more charge-transfer bands, since this favors *trans* to *cis* isomerization under visible light excitation.

Illumination of azobenzene compounds in the liquid phase, and sometimes in solid media, results in *trans* to *cis* isomerization until reaching a photostationary state. This transformation is usually accompanied by an increase in intensity of the longer-wavelength absorption profile and a noticeable blue shift.[26] Both observations are explained by the elevated oscillator strength for the *cis* isomer and the concomitant increase in energy between the n–π* levels. Visible-light irradiation of **AZV** in aerated (or N_2-purged) CH_3CN led to significant changes in the absorption spectrum (see Supple-

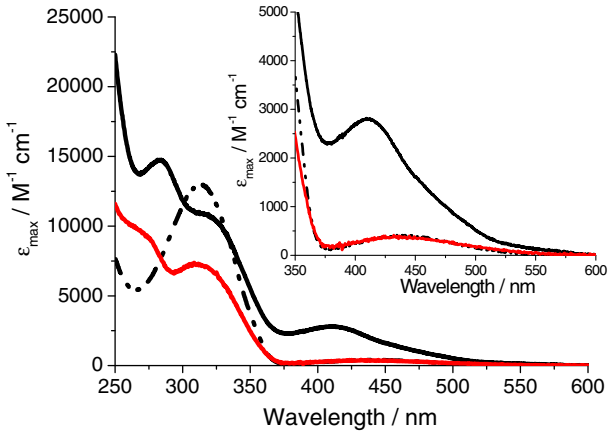

Figure 5. Room temperature absorption spectrum for **AZV** (—) methyl ester **5** (-·-) and compound **3** (▬) in dry CH_3CN. Insert shows the expansion of the longer-wavelength absorption profiles.

mentary data). In particular, the intensity of those bands centered at 411, 316 and 283 nm diminished gradually during photolysis, but reached a steady-state value after some 30 min or so (see Supplementary data). There is also a modest blue-shift and line-narrowing for the lower-energy absorption band. After photolysis, the absorption profile shows signs of partial recovery over a few hours but on prolonged standing in the dark it becomes clear a new species was formed. A similar experiment performed on **5** in aerated CH_3CN resulted in the expected blue-shift and increase in intensity to the absorption band centered at 442 nm. Rather surprisingly, no major changes to the absorption spectrum occurred after leaving the sample in the dark for several hours (see Supplementary); after 3 days a shoulder appeared on the longer-wavelength band. Prior work by Joshua et al.[27] concluded that irradiation of **5** in 1,2-dichloroethane results in no permanent change to the molecule, and that the observed color change arises from *trans* to *cis* isomerization. Our findings suggest, however, that the overall behavior is more complex. It would appear that *trans* to *cis* isomerization of the azobenzene unit does take place upon illumination of **AZV**, but this is followed by secondary events that lead, in part, to decomposition of the compound.

Although alkylation products of **4** could not be isolated pure, photoisomerization of the basic cyclophane was tested in CH_2Cl_2 and 2-MeTHF. Illumination of either solution with white light resulted in no real appreciable change in the UV–visible spectrum (see Supplementary data). It is possible that a single or concerted isomerization of the azobenzene groups is too difficult, or that the thermal *cis* to *trans* isomerization rate is fast. Even so, the computed cyclophane structure reveals existence of a highly oxygen-rich central cavity consummate for binding metal ions. We expect to explore this type of chemistry, especially with lanthanide ions.

A prototypic light-activated variable resistor has been designed and synthesized as part of this work. A key finding is that the compact azobenzene–viologen cyclophane can be assembled by way of a simple esterification reaction, although both [1+1] and [2+2] products appear. Stable products emerging from the subsequent N-alkylation of the 4,4′-bipyridine unit are found only for the smaller cyclophane, with the resultant dicationic species being subjected to considerable internal strain. Part of the design rationale for this system revolved around the desire to twist the viologen subunit by way of light-activated *trans* to *cis* isomerization at the corresponding azobenzene unit. Unfortunately, internal strain is so severe that it disturbs both subunits. A direct consequence of this effect is that the mono-cation formed on electrochemical reduction of the viologen is unable to adopt a planar geometry and undergoes a competing chemical reaction that relieves the steric strain. Somewhat surprisingly given this behavior, photo-induced *trans* to *cis* isomerization is observed for the target cyclophane, raising the possibility to study the electrochemical behavior of the *cis* form by cyclic voltammetry. Such studies are currently in progress and will be reported at a later date.

Acknowledgments

This work was supported by the Engineering and Physical Sciences Research Council (EPSRC EP/G0409X/1 and EP/F03637X/1). The EPSRC-sponsored Mass Spectrometry Service at Swansea is also thanked for collecting the mass spectra of certain compounds.

Supplementary data

Supplementary data (a selection of cyclic voltammograms recorded for AZV and methyl ester 5 at different scan rates. DFT calculation results, fitted spectra and absorption spectra for AZV, 4 and 5 after irradiation with white light) associated with this article can be found, in the online version, at doi:10.1016/j.tetlet.2011.08.013.

References and notes

1. Benniston, A. C.; Mackie, P. R. In *Nanostructured Materials and Nanotechnology*; Nalwa, H. S., Ed.; Academic Press: London, 2002; pp 693–747.
2. Shinkai, S.; Yoshioka, A.; Nakayama, H.; Manabe, O. *J. Chem. Soc., Perkin Trans. 2* **1990**, 1905–1909.
3. Kikuchi, J.; Egami, K.; Suehiro, K.; Murakami, Y. *Chem. Lett.* **1992**, 1685–1688.
4. Amabilino, D. B.; Dietrich-Buchecker, C. O.; Livoreil, A.; Pérez-García, L.; Sauvage, J.-P.; Stoddart, J. F. *J. Am. Chem. Soc.* **1996**, *118*, 3905–3913.
5. Ashton, P. R.; Balzani, V.; Becher, J.; Credi, A.; Fyfe, M. C. T.; Mattersteig, G.; Menzer, S.; Nielsen, M. B.; Raymo, F. M.; Stoddart, J. F.; Venturi, M.; Williams, D. J. *J. Am. Chem. Soc.* **1999**, *121*, 3951–3957.
6. Benniston, A. C.; Harriman, A.; Lynch, V. M. *J. Am. Chem. Soc.* **1995**, *117*, 5275–5291.
7. Dvomikovs, V.; House, B. E.; Kaetzel, M.; Dedman, J. R.; Smithrud, D. B. *J. Am. Chem. Soc.* **2003**, *125*, 8290–8301.
8. Jeppesen, J. O.; Nielsen, K. A.; Perkins, J.; Vignon, S. A.; Di Fabio, A.; Ballardini, R.; Gandolfi, M. T.; Venturi, M.; Balzani, V.; Becher, J.; Stoddart, J. F. *Chem. Eur. J.* **2003**, *9*, 2982–3007.
9. Fioravanti, G.; Haraszkiewicz, N.; Kay, E. R.; Mendoza, S. M.; Bruno, C.; Marcaccio, M.; Wiering, P. G.; Paolucci, F.; Rudolf, P.; Brouwer, A. M.; Leigh, D. A. *J. Am. Chem. Soc.* **2008**, *130*, 2593–2601.
10. Balzani, V.; Credi, A.; Venturi, M. *Chem. Soc. Rev.* **2009**, *38*, 1542–1550.
11. Barrett, C. J.; Mamiya, J.; Yager, K. G.; Ikeda, T. *Soft Matter* **2007**, *3*, 1249–1261.
12. Benniston, A. C. *Chem. Soc. Rev.* **2006**, *25*, 427–435.
13. Yager, K. G.; Barrett, C. J. *J. Photochem. Photobiol. A Chem.* **2006**, *182*, 250–261.
14. Mativetsky, J. M.; Pace, G.; Elbing, M.; Rampi, M. A.; Mayor, M.; Samori, P. *J. Am. Chem. Soc.* **2008**, *130*, 9192–9193.
15. Bockman, T. M.; Kochi, J. K. *J. Org. Chem.* **1990**, *55*, 4127–4135.
16. Benniston, A. C.; Harriman, A.; Li, P.; Rostron, J. P.; Harrington, R. W.; Clegg, W. *Chem. Eur. J.* **2007**, *13*, 7838–7851.
17. Zhang, C.; He, Y.; Cheng, H.-P.; Xue, Y.; Ratner, M. A.; Zhang, X.-G.; Krstic, P. *Phys. Rev. B* **2006**, *73*, 125445-1–125455-5.
18. Benniston, A. C.; Harriman, A.; Li, P.; Rostron, J. P. *Tetrahedron Lett.* **2005**, *46*, 7291–7293.
19. Doumit, C. J.; McPherson, G. L.; Belford, R. L.; Lanoux, S. B.; Janassen, H. B. *Inorg. Chem.* **1977**, *16*, 565–569.
20. *Data for* ***3***: ^{1}H NMR (300 MHz, $CDCl_3$): δ = 8.70 (2H, s), 8.55 (2H, d, J = 4.6 Hz), 7.87 (2H, dd, J = 7.8, 1.4 Hz), 7.68 (2H, dt, J = 7.8, 1.4 Hz), 7.54 (2H, dd, J = 8.0, 1.2 Hz), 7.50 (2H, dt, J = 7.6, 1.4 Hz), 7.29 (2H, d, J = 5.0 Hz). ^{13}C NMR ($CDCl_3$): δ = 164.7, 153.3, 147.5, 144.8, 144.5, 136.0, 133.8, 131.7, 130.2, 125.5, 124.0, 121.8; HRMS (NSI) found: 423.1088 $[M+H]^+$, $C_{24}H_{15}O_8N_4$ requires: 423.1088.
21. *Data for* ***4***: ^{1}H NMR (300 MHz, $CDCl_3$): δ = 8.73 (4H, d, J = 4.8 Hz), 8.66 (4H, s), 7.64 (4H, dd, J = 7.7, 1.4 Hz), 7.49 (4H, d, J = 4.8 Hz), 7.32 (4H, dt, J = 7.7, 1.2 Hz), 7.21 (4H, dt, J = 7.7, 1.2 Hz), 6.91 (4H, dd, J = 8.0, 1.2 Hz); HRMS (NSI) found: 845.2104 $[M+H]^+$, $C_{48}H_{29}O_8N_8$ requires: 845.2103.
22. Engbersen, J. F. J.; Geurtsen, G.; De Bie, D. A.; Van der Plas, H. C. *Tetrahedron* **1988**, *44*, 1795–1802.
23. *Data for* ***AZV***: ^{1}H NMR (300 MHz, $CDCl_3$): δ = 9.09 (2H, s), 8.67 (2H, d, J = 6.4 Hz), 8.09 (2H, d, J = 6.3 Hz), 7.88 (2H, dd, J = 7.7, 1.3 Hz), 7.84 (2H, dt, J = 7.1, 1.4 Hz), 7.79 (2H, dd, J = 8.0, 1.3 Hz), 7.66 (2H, dt, J = 7.5, 1.4 Hz), 4.36 (s, 6H). ^{13}C NMR ($CDCl_3$): δ = 164.3, 152.6, 147.4, 144.1, 141.6, 141.5, 135.5, 132.2, 132.1, 130.9, 124.2, 123.2, 50.2. ^{19}F NMR ($CDCl_3$): δ = −79.3. HRMS (NSI) found: 601.0985 $[M-CF_3SO_3]^+$, $C_{27}H_{20}F_3N_4O_7S_1$ requires: 601.0999. Elemental analysis found C, 45.53; H, 3.57; N, 6.84, $C_{28}H_{20}F_6N_4O_{10}S_2.Et_2O$ requires C, 46.60; H, 3.67; N, 6.79. For partial solvate $C_{28}H_{20}F_6N_4O_{10}S_2.0.5\ Et_2O$ C, 45.75; H, 3.20; N, 7.11.
24. *Selected X-ray data*: $C_{32}H_{30}F_6N_4O_{11}S_2$; 824.72; a = 11.6190(7), b = 11.9384(6), c = 13.8669(8); α = 76.073(5)°, β = 73.957(5)°, γ = 71.458(5)°; V = 1727.82(17) Å^3; Z = 2; F(0 0 0) = 848; R indices [$F^2 > 2\sigma$] $R1$ = 0.0537, w$R2$ = 0.1463; R indices (all data) $R1$ = 0.0721, w$R2$ = 0.1585. Crystallographic data (excluding structure factors) for the structures in this paper have been deposited with the Cambridge Crystallographic Data Centre as supplementary publication no. CCDC 827803. Copies of the data can be obtained, free of charge, on application to CCDC, 12 Union Road, Cambridge CB2 1EZ, UK, (fax: +44-(0)1223-336033 or e-mail: deposit@ccdc.cam.ac.Uk).
25. Lednev, I. K.; Ye, T.-Q.; Matousek, P.; Towrie, M.; Foggi, P.; Neuwahl, F. V. R.; Umapathy, S.; Hester, R. E.; Moore, J. N. *Chem. Phys. Lett.* **1998**, *290*, 68–74.
26. Birnbaum, P. P.; Linford, J. H.; Style, D. W. G. *Trans. Faraday Soc.* **1953**, *49*, 735–744.
27. Joshua, C. P.; Rajasekharan Pillai, V. N. R. *Tetrahedron Lett.* **1973**, *37*, 3559–3562.